New Journal of Physics
The open access journal at the forefront of physics
Deutsche Physikalische Gesellschaft DPG | IOP Institute of Physics

Characterization of laser-driven single and double electron bunches with a permanent magnet quadrupole triplet and pepper-pot mask

G G Manahan, E Brunetti, C Aniculaesei, M P Anania, S Cipiccia, M R Islam, D W Grant, A Subiel, R P Shanks, R C Issac, G H Welsh, S M Wiggins and D A Jaroszynski[1]

Scottish Universities Physics Alliance, Department of Physics, University of Strathclyde, Glasgow G4 0NG, UK
E-mail: d.a.jaroszynski@strath.ac.uk

Received 13 May 2014, revised 6 August 2014
Accepted for publication 5 September 2014
Published 7 October 2014

New Journal of Physics **16** (2014) 103006

doi:10.1088/1367-2630/16/10/103006

Abstract

Electron beams from laser-plasma wakefield accelerators have low transverse emittance, comparable to those from conventional radio frequency accelerators, which highlights their potential for applications, many of which will require the use of quadrupole magnets for optimal electron beam transport. We report on characterizing electron bunches where double bunches are observed under certain conditions. In particular, we present pepper-pot measurements of the transverse emittance of 120–200 MeV laser wakefield electron bunches after propagation through a triplet of permanent quadrupole magnets. It is shown that the normalized emittance at source can be as low as $1\,\pi$ mm mrad (resolution limited), growing by about five times after propagation through the quadrupoles due to beam energy spread. The inherent energy-dependence of the magnets also enables detection of double electron bunches that could otherwise remain unresolved, providing insight into the self-injection of multiple bunches. The combination of quadrupoles and pepper-pot, in addition, acts as a diagnostic for the alignment of the magnetic triplet.

Keywords: emittance, permanent quadrupoles, laser wakefield accelerators

[1] Author to whom any correspondence should be addressed.

1. Introduction

Laser-wakefield accelerators (LWFAs) are table-top devices capable of delivering high quality electron beams with energies up to GeV levels by exploiting the large electric field gradients created when intense laser pulses interact with plasma [1]. The small size of the accelerator and the promising properties of electron beams make LWFAs attractive tools in many fields, including as potential drivers of a new generation of compact synchrotron-like [2–4] and free-electron laser (FEL) [5–7] light sources. The requirement of such applications to transport beams over long distances with minimum degradation has prompted the development of beam lines and diagnostic systems tailored for laser-produced beams, which so far suffer from larger instabilities than conventional radio frequency (RF) accelerators. To avoid electron beam blow-up over long drift propagation, miniature permanent magnet quadrupole (PMQ) lenses are typically installed close to the accelerator [6, 7]. These have very high magnetic field gradients ($\sim 500\,\mathrm{T\,m^{-1}}$) for collimation and focusing of high energy beams over short distances. Design, fine tuning and beam transport capabilities of the PMQs have been studied in detail [8, 9], leading to further control of the electron beam divergence and pointing stability [10].

The quality of a particle beam is best defined by the transverse emittance, a measure of the phase-space volume occupied by the particles and a figure-of-merit for the beam focusability, as well as for the brightness of potential radiation sources. Direct and indirect measurements have shown that the transverse normalized emittance of LWFA beams can be as low as $0.2\,\pi$ mm mrad [11–13], comparable with RF accelerators. In this paper, we present a pepper-pot mask-based diagnostic system for the characterization of laser-produced electron beams after propagation through a triplet of PMQs. We show that this system can measure transverse emittance down to $1\,\pi$ mm mrad both at the source and after propagation through the quadrupoles, limited by the detection system resolution. It can also be used to characterize the magnetic field gradient and the alignment of strong PMQs, parameters that are difficult to measure due to the small size and high gradients of the magnets [8, 9].

Furthermore, the versatility of combining quadrupoles with the pepper-pot can provide insight into the occurrence of double electron bunches in a single shot. The generation of more than one bunch can either be due to injection instability (as shown in the modulated electron spectra in figure 1 for our beam line, it is indeed a common feature of many reported experiments [14–16]) or deliberated (driven, for example, by colliding pulse injection [17] or oscillating bunch injection [18]) that may itself lead to future exploitation of ultrashort electron bunch trains. In the former case, it is particularly prevalent for near-threshold self-injection [19] and is a significant outcome of shot-to-shot fluctuations in the LWFA that require better understanding and control. Certain properties of multiple electron bunches can be extracted from electron energy spectra [14–16] and transition radiation spectra (energy, temporal separation) [17, 19] measurements. We show that the PMQ/pepper-pot system can resolve electron bunches of equal energy if their pointing angles are sufficiently different because of different transverse momenta of each bunch, and the wake dynamics [20].

This paper is arranged as follows: section 2 discusses LWFA beam propagation using quadrupole magnets. Section 3 introduces the pepper-pot emittance technique and its coupling to the PMQs. Section 4 describes the experimental methods. The results are presented in section 5, where measurements of double bunches are presented, and conclusions drawn in section 6.

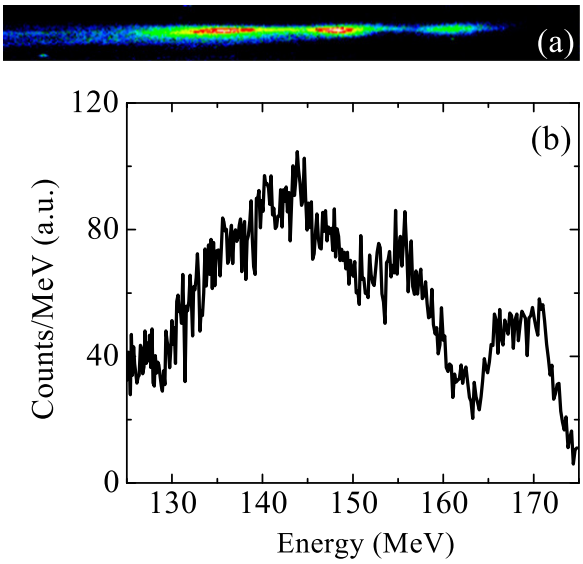

Figure 1. An electron energy spectrum with (a) false colour screen image and (b) signal line-out showing three distinct bunches as captured on the ALPHA-X beam line (details given in section 4).

2. Transporting LWFA electron beams with quadrupole magnets

Electron bunches exiting the plasma accelerator have an inherent beam divergence (typically a few mrad) [1] so that external collimation or focusing is often required for beam application. Magnetic quadrupoles are focusing elements where the magnetic fields linearly increase with the distance from the axis. If the effective length, l_{ef}, of a quadrupole is much smaller than its focal length, f, then it can be treated as a thin lens, and the focal length can be expressed using $1/f = kl_{ef}(ec/E)$, where k is the magnetic strength, c is the vacuum speed of light and e and E are the electron charge and energy respectively [21]. If the quadrupole field is produced by permanent magnets, then its focusing strength decreases with beam energy. A single quadrupole focuses the beam in one plane and defocuses in the other plane, therefore, a series of quadrupoles are often designed to produce a lens system that focuses the beam in both planes. A common example is a triplet, where three quadrupoles are combined in series with alternating focusing directions and separated by drift distances, to produce strong symmetric focusing [8].

A PMQ triplet is highly advantageous for LWFA beam lines because they are very compact yet capable of effectively transporting bunches with GeV-scale energy [22]. One has recently been implemented on our beam line for bunch propagation through an undulator as part of a programme to develop a vacuum ultra-violet FEL light source [7]. Similar work elsewhere in the extreme ultra-violet spectral range has employed a PMQ doublet [6]. Depending on the separation distance, a PMQ triplet is capable of focusing the beam down to a few microns for a specific energy. However, a spread of focal points results for electron bunches that have a non-zero energy spread, a typical property of LWFA electron beams. This results in distortion of the phase space ellipse of the beam and, therefore, an increase in the projected emittance.

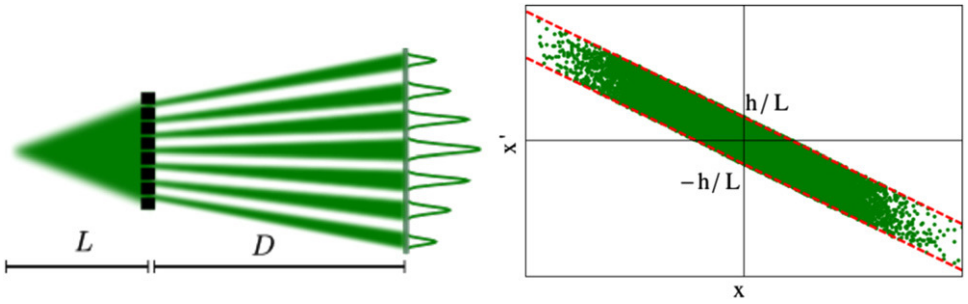

Figure 2. Phase-space region (x, x') selected by an aperture with radius h placed at a distance L from a particle source with transverse Gaussian distribution.

3. Pepper-pot mask emittance technique with PMQs

The transverse properties of a particle beam can be probed by measuring the beamlet pattern produced after propagation through a mask consisting of an array of small holes drilled in a material capable of stopping or deflecting particles, as shown schematically in figure 2. A beam with source size and divergence of σ and σ', respectively, and with initial transverse distribution

$$\mathscr{P}(x, x') = \exp\left(-\frac{1}{2}\frac{x^2}{\sigma^2}\right)\exp\left(-\frac{1}{2}\frac{x'^2}{\sigma'^2}\right) \tag{1}$$

passing through an aperture with radius h centered at $x = y = 0$ is converted into a beamlet sampling a small sub-region of phase-space. Assuming that $\sigma, h \ll \sigma_{\mathrm{m}}$, where $\sigma_{\mathrm{m}} = \sqrt{\sigma^2 + L^2\sigma'^2}$ is the beam size on the mask and L is the distance between source and mask, the beamlet rms size and divergence are $\sigma_b = \sigma$ and $\sigma'_b = \sqrt{\sigma^2 + h^2/3}\big/L$, respectively. After a drift distance D from the mask, the beamlet final size is

$$\sigma_{b,f} = \left(M - \frac{\sigma^2}{\sigma^2 + h^2/3}\right)\sqrt{\sigma^2 + \frac{h^2}{3}}\ , \tag{2}$$

with $M = (D + L)/L$ the system magnification. For small angles, this formula also applies to beamlets propagating off-axis, which are ideally centred on a grid with separation Md, with d the hole spacing in the mask. A measurement of the charge, position and size of the beamlet pattern allows reconstruction of the phase-space distribution of a generic beam, and therefore the beam emittance [23].

When focusing elements, such as a PMQ triplet, are placed between source and mask, the beamlet size and separation also depends on the beam energy, an effect that can be described using simple analytical formulae by treating magnetic quadrupoles as thin lenses, an approximation, however, that is not very accurate for compact high gradient magnets. With this assumption, a system of several lenses can be described by a compound focal length $F = F(E)$ preceded and followed by two drift sections with length A and B respectively, where F is a function of the gradient and separation of the magnets, as well as of the beam energy [21]. A beam exiting such a system is equivalent to the output of a virtual particle source with size, σ_{v}, and divergence, σ'_{v}

$$\sigma_{\mathrm{v}} = \left[\frac{F(E)}{(F(E)+A)^2 + \sigma^2/\sigma'^2}\right]\sigma \tag{3}$$

$$\sigma'_{\mathrm{v}} = \left[\frac{(A+F(E))^2 + \sigma^2/\sigma'^2}{F(E)}\right]\sigma', \tag{4}$$

which is displaced by a distance L_{v}

$$L_{\mathrm{v}} = \frac{[F(E)+A]^2 B + [F(E)+A]AF(E) + [F(E)+B]\sigma^2/\sigma'^2}{(F(E)+A)^2 + \sigma^2/\sigma'^2} \tag{5}$$

from the real source position, implying that particles with different energies will have different magnification, i.e. $M = M(E)$. If particles emitted by such a source are filtered through a pepper-pot mask, the divergence, position and size of the resulting beamlets become strongly dependent on the characteristics of the focusing system and on the beam energy, making this device a useful diagnostic for both electron beams and magnetic elements. For instance, beamlets with different energies will produce different beamlet separation on the detecting screen.

The system composed of pepper-pot mask and PMQ triplet has been modelled using GEANT4 [24], simulating the beamlet distribution on a Ce:YAG scintillating crystal for a resolution of 10 μm and different electron beam parameters. When focusing elements are not used, changes in beamlet size indicate changes in the transverse source size. When quadrupoles are used, however, longitudinal and transverse properties are coupled and beamlet size and shape depend not only on the transverse emittance, but also on the energy spread and beam pointing. Figure 3(a) shows that for energy spreads smaller than 1–2% and on-axis propagation, the beamlet size is mostly determined by the transverse source size, with GEANT4 results matching the analytical curves obtained by treating quadrupoles as simple lenses. For large energy spreads and off-axis propagation (figure 3(b)), however, the beamlet size grows quickly due to the chromaticity of the quadrupoles. Electrons exiting the triplet appear to be emitted from a virtual point source located further back than the real accelerator position by an amount dependent on the beam energy. The resulting beamlets are thus the convolution of many virtual sources located at different positions and become broader and distorted. This effect can be so severe as to make off-axis beamlets undetectable, as shown in the simulated pepper-pot images of figure 4 for 0.8 pC and 2.5 mrad beams. Therefore, for charges of the order of $\simeq$1 pC the setup employed here can directly measure the emittance after the triplet only when the energy spread is smaller than 1–2% and the divergence is of the order of $\simeq$1 mrad.

Neverthless, if the beam divergence is known from independent measurements and the particle distribution is approximately Gaussian, the emittance before and after the quadrupoles can be indirectly measured by subtracting the contribution of energy spread and pointing angle from the beamlet size. The energy spread can be obtained from separate measurements or can be estimated from the beamlet distribution, since beamlets located off-axis are broadened more than beamlets close to the centre. For the electron energies and PMQ configuration considered here, the beam central energy does not affect significantly the beamlet size, but it changes the beamlets' separation.

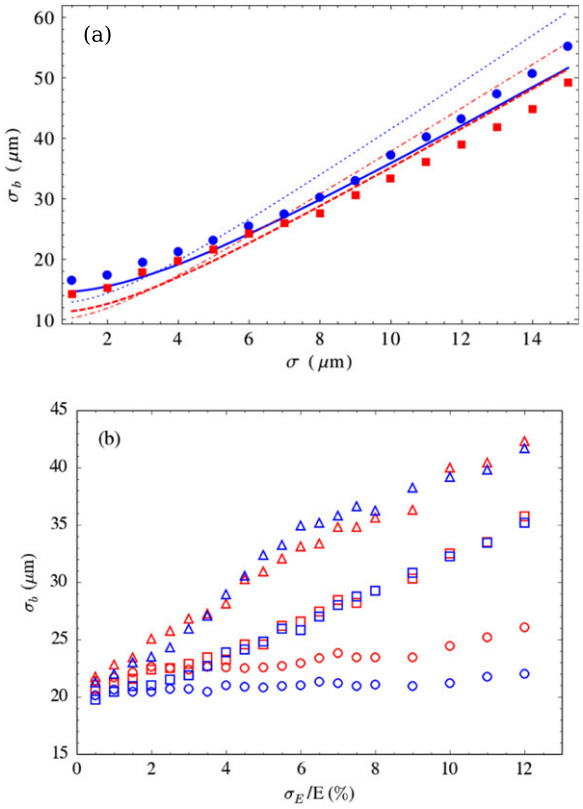

Figure 3. Beamlet size (a) versus source size with $\sigma_E/E = 1\%$ and (b) versus σ_E/E with normalized $\epsilon_{\text{rms}} = 1\pi$ mm mrad for electron beams passing through a PMQ triplet and pepper-pot mask with properties matching the experimental setup shown in figure 5. In both figures, blue is for horizontal axis (which is in a defocusing–focusing–defocusing (DFD) configuration), while red is for vertical axis (which is in focusing–defocusing–focusing (FDF) configuration). In (a) the circle and square symbols are the results of numerical simulations performed using GEANT4, the solid and dashed lines correspond to analytical calculations for thick quadrupoles, and the dotted and dot-dashed lines use the thin-lens approximation. In (b) the symbols correspond to beamlets located at different positions in the pepper-pot image simulated using GEANT4-circle: on-axis/centre, square: second beamlet from the centre, triangle: third beamlet from the centre.

4. Experimental methods

Experiments for the characterization of laser-produced electron beams using a PMQ triplet coupled to a pepper-pot mask have been performed at the Advanced Laser-Plasma High-energy Accelerators towards X-rays (ALPHA-X) beam line [3] with the setup shown in figure 5. The laser delivers 35 fs, 800 nm pulses with 900 mJ of energy on target. After focusing to a 20 μm ($1/e^2$ radius) vacuum spot size by an $f/18$ spherical mirror, the peak intensity reaches 2×10^{18} W cm^{-2}, corresponding to a normalized vector potential $a_0 \sim 1$. The laser interacts with a supersonic helium gas jet generated by a nozzle with the following geometrical parameters: 0.5 mm throat diameter, 2 mm outlet and 16.7 semi-opening angle. The plasma density at the laser focus, assuming full ionization is of the order of 2–3 $\times 10^{19}$ cm^{-3}. The accelerator typically

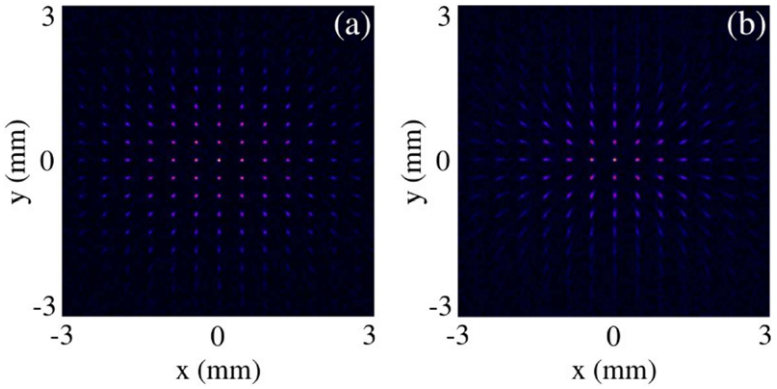

Figure 4. Simulated pepper-pot images for an electron beam with initial normalized emittance of $4\,\pi$ mm mrad and rms energy spread of (a) 3% and (b) 7%.

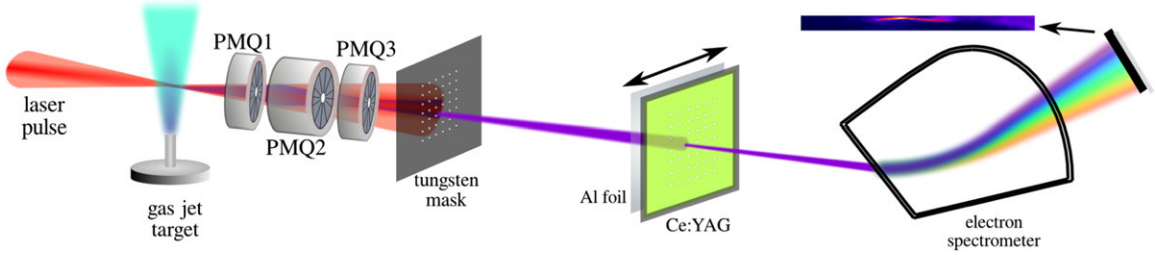

Figure 5. Schematic diagram for electron beam characterization by combining the pepper-pot technique and PMQ triplet. The distance from the accelerator to the emittance mask is 30 cm. The PMQ triplet is located 10.4 cm (measured from the centre of the triplet) from the accelerator. Pepper-pot spots are detected on the Ce:YAG crystal 70 cm after the mask. Energy spectra are separately measured using a magnetic dipole imaging spectrometer, located 259 cm from the accelerator.

produces electron beams with rms (single peak) energy of 125 ± 10 MeV (with energy jitter of 10%), rms divergence of 2–3 mrad and charge up to 2 pC. Energy spectra have been diagnosed using a magnetic dipole imaging spectrometer (field strength of 0.5 T) [25] with Ce:YAG screen imaged by a 12-bit charge-coupled device (CCD) camera and charge has been determined with Fuji BAS image plates [26].

The PMQ triplet is placed at a distance of 10.4 cm from the accelerator (measured from the centre of the triplet) and can be remotely inserted in and out of the beam line. The gradients are approximately $k_1 = 422\,\mathrm{T\,m^{-1}}$, $k_2 = 446\,\mathrm{T\,m^{-1}}$, $k_3 = 422\,\mathrm{T\,m^{-1}}$ and the quadrupole separation is $A = B = 33 \pm 1$ mm. The first (PMQ1) and third (PMQ3) quadrupole are arranged to focus the electron beam in the vertical axis, with the second quadrupole (PMQ2) defocusing it. The reverse behaviour is obtained in the horizontal direction. The electron beam transverse profile is detected on a 2×2 cm Ce:YAG screen with a thickness of $150\,\mu$m placed at a distance of 100 cm from the accelerator and imaged by a 14 bit CCD camera, with an overall spatial resolution of $10\,\mu$m. A pepper-pot mask consisting of a $125\,\mu$m thick tungsten sheet pierced by a 54×54 array of $16 \pm 2\,\mu$m diameter holes (pitch $= 142 \pm 2\,\mu$m) can be inserted at a distance of 30 cm from the gas jet. Electrons passing through the holes form small beamlets that drift to the Ce:YAG screen, whereas those hitting the mask are scattered, adding a uniform background which can be

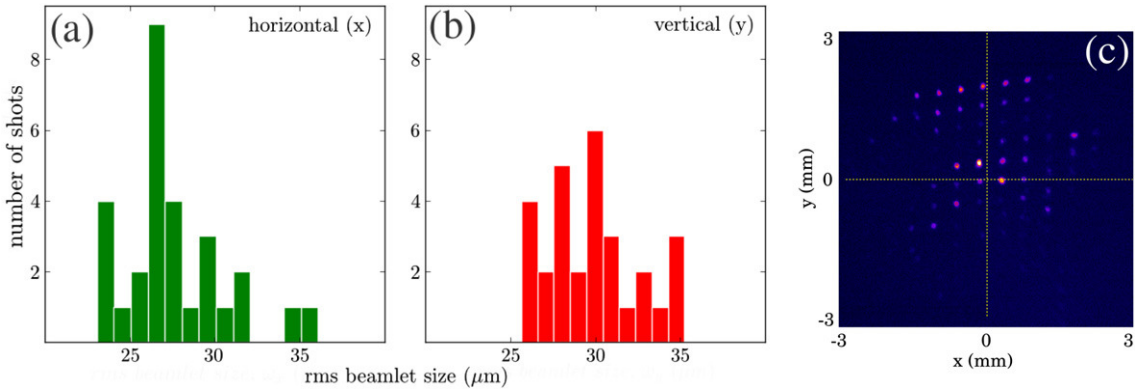

Figure 6. Distribution of the measured smallest beamlet size in the (a) horizontal and (b) vertical planes for 28 consecutive laser shots after propagation through the PMQ triplet. An example of a false colour pepper-pot image as detected by the Ce:YAG screen is also shown (c).

removed from the recorded images after processing. For the chosen quadrupole separation, electron beams with energy of ∼90 MeV are collimated to sizes too small to produce useful beamlet patterns for the hole separation of the mask used here. At higher energies, the magnetic strengths of the PMQs are weaker, and therefore the beam divergence is only reduced, allowing the production of a sufficient number of beamlets after the beam is filtered through the mask.

5. Results and discussions

The distribution of the smallest measured beamlet sizes (σ_b) for 28 pepper-pot images recorded in this experiment is shown in figure 6, reporting an average value of $30 \pm 4\,\mu$m in both x and y. The electron beam rms divergence measured from an average of 100 consecutive shots with no mask and no PMQs is $\sigma_{x',\mathrm{rms}} = 2.2$ mrad and $\sigma_{y',\mathrm{rms}} = 2.7$ mrad, with the beam emitted ∼1 mrad off-axis. Taking into account the ∼5 μm beamlet size growth caused by energy spread ($\sigma_E/E \sim 8\%$) and pointing fluctuations, the estimated source size based on figure 3 is between 2 and 5 μm. Using the divergence measured separately and the estimated source size, the corresponding initial emittance is between 1 and 4 π mm mrad. Considering these experimental parameters, the simulations from GEANT4 predicted that the transverse projected emittance grows five times after propagating through the PMQ triplet, between 5 and 20 π mm mrad for beam emitted approximately on-axis, due to non-zero energy spread.

Pepper-pot emittance measurements with no PMQs have been performed in the same conditions, obtaining horizontal and vertical normalized emittances $\epsilon_{\mathrm{rms},x,y} = 1.6 \pm 0.5$ π mm mrad from an average of 20 shots, confirming the source size estimated from pepper-pot measurements with PMQ triplet.

The presence of the quadrupoles leads to an energy dependence of the detection system magnification, M, as shown in equations (3)–(5). The calculated magnification of the pepper-pot system coupled with the PMQ triplet is given in figure 7 as a function of electron energy with the system magnification without the PMQs indicated by the dashed line for reference. As a result, a variation of the beamlets separation with energy is captured on the Ce:YAG screen. For instance, if double bunches pass through the PMQ triplet and the mask, two beamlet alignments

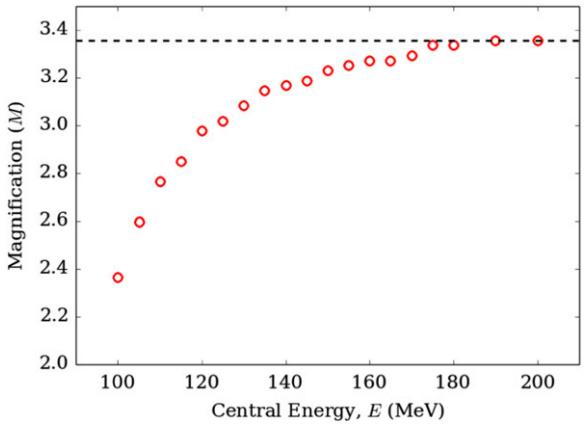

Figure 7. Magnification of the pepper-pot coupled with PMQ triplet imaging system as a function of energy. The horizontal dashed line indicates the system magnification without the PMQ triplet.

are visible on the image. Among the recorded pepper-pot images, around 10% display this unique behaviour and examples are shown in figure 8.

To emphasize the two distinct arrangements of beamlets, the most prominent portions are also shown in close-up and two different sets of guide lines (red and white) are traced. In figure 8(a), the measured distance between the red lines is $d_{r,1} = 406 \pm 11\ \mu$m, giving a magnification of $M_{r,1} = 2.8 \pm 0.1$; while $d_{w,1} = 455 \pm 19\ \mu$m for the white lines, equivalent to $M_{w,1} = 3.2 \pm 0.2$. Based on expected electron beam propagation through the triplet (figure 7), the two electron central energies corresponding to these magnifications are estimated to be ~120 MeV (for $M_{r,1}$) and between 140 and 160 MeV (for $M_{w,1}$). The difference between $d_{r,1}$ and $d_{w,1}$ is only visible in the central region of the beamlets distribution, implying that the two electron bunches are emitted at the same angle but one bunch has larger divergence, i.e. the scenario depicted is dominated by the energy difference with small pointing angle difference. The integrated charges for the two bunches are 48% (red lines) and 52% (white lines) from the total charge of all resolvable beamlets. A fitted transverse profile of such electron bunches distribution is shown in the lower inset of figure 8(a).

A converse scenario is depicted for the two traces of figure 8(b) where the measured separations agree to within the experimental uncertainty: $d_{r,2} = 481 \pm 7\mu$m ($M_{r,2} = 3.4 \pm 0.1$) for the red lines and $d_{w,2} = 462 \pm 16\mu$m ($M_{w,2} = 3.3 \pm 0.2$) for the white lines. The relative bunch charges in this case are 42% (red lines) and 58% (white lines). The similarity of the magnification values indicates that the difference in the central energies of two electron bunches is small. It is estimated that the electron bunches producing these beamlets have energies ranging between 160 and 200 MeV. Simulations indicate that for the current PMQ triplet assembly, different beamlet separation is recognizable when the two bunches are separated by $\geqslant$30 MeV, independent of the central energy. Bunches separated by less than 30 MeV are not normally resolvable and will produce beamlets similar to a single bunch with large energy spread. However, the distinction in figure 8(b) becomes visible since it is dominated by the pointing angle difference of the two bunches (2 mrad in both transverse planes), producing two separate beam trajectories as the bunches exit the PMQ triplet. This consequence would still apply for bunches of precisely equal energy. The transverse profile of electron bunches fitted for this condition is shown in the lower inset of figure 8(b).

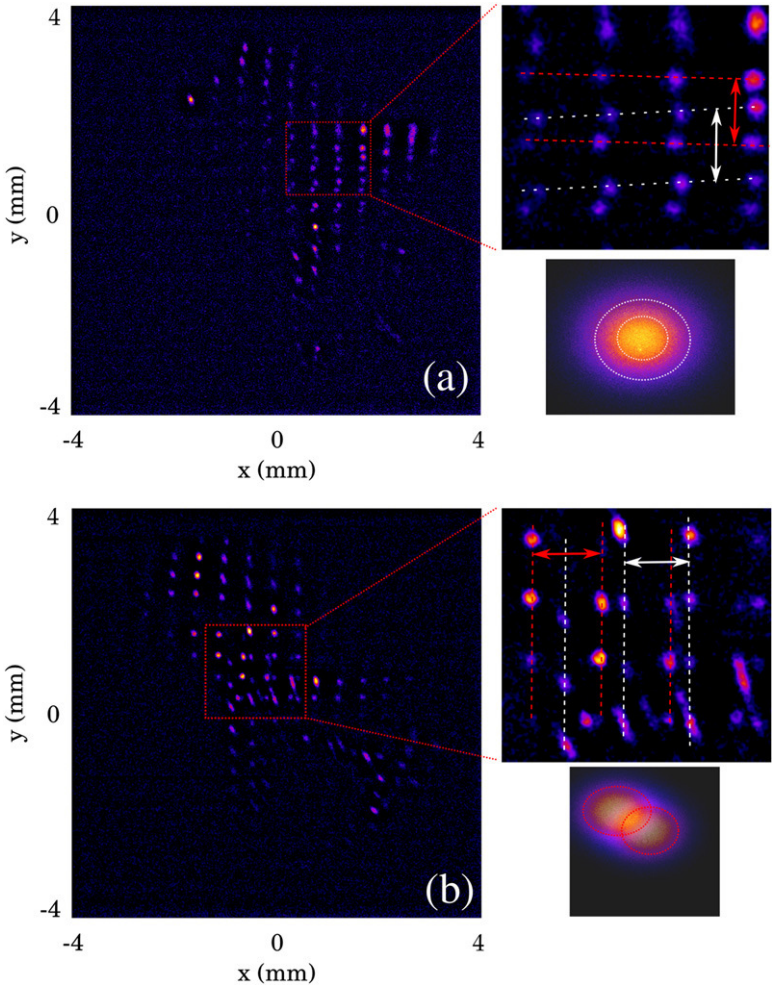

Figure 8. False colour pepper-pot images measured after propagation through the PMQ triplet and showing double beamlet structure for (a) spatially overlapping bunches and (b) bunches with different pointing angles. Each figure has an upper inset depicting a zoomed-in (3×) portion of the image indicating two different beamlets arrangements (red and white dotted lines). Lower insets show the respective fitted transverse profile of the electron bunches.

Our measurements illustrate some of the consequences of the fluctuating nature of electron self-injection. The effect of the combined pepper-pot/PMQ triplet allows double bunches, with either different energy or pointing angle, to be distinguished. In principle, more than two distinct bunches can be resolved if sufficient numbers of disparate beamlets are imaged. For the experimental conditions of the ALPHA-X accelerator, electron bunches are self-injected after relativistic and ponderomotive self-focusing of the laser pulse [27] in the upward plasma density ramp at the entrance of the gas jet. Self-injection occurs near threshold for injection, which is consistent with the low total charge (~few pC) observed. Electron charge build-up at the rear of the bubble due to bubble sheath current crossing governs injection, which leads to a series of ultra-short electron bunches [19]. Under these conditions, the injected charge and bunch temporal structure are sensitive to small changes in both the laser intensity, chirp, phase-front etc, and the plasma parameters (density, entrance ramp, etc). Multiple electron bunches

arise from repeated self-injection because of the fluctuating bubble potential and injection threshold. As a result, a set of beamlets can be formed (figure 8) and structured electron spectra can arise (figure 1), following acceleration in the bubble. The bunch charge can be comparable in each set of beamlets, as shown in figure 8. The bunch energy also depends strongly on where injection occurs in the gas jet, which can result in set of beamlets having significantly different energies. Double bunches of differing energy are most likely produced in the same bubble, with the first injected bunch undergoing more acceleration than the second (figure 8(a)). Furthermore, the bunches can have different amounts of transverse momentum, which results in different pointing angles for the bunches. Significant transverse momentum of electron bunches undergoing betatron oscillation can be acquired through harmonic resonant betatron coupling to the laser field, which partially fills the bubble [4]. This can result in a relatively large pointing angle and pointing angle fluctuations at the exit of the accelerator.

The combination of PMQs and pepper-pot mask can also detect rotational misalignment of the PMQ triplet assembly. Misalignment is undesirable because a rotated magnetic field degrades the performance of the triplet as a focusing system and induces additional transverse emittance growth. A well-aligned magnetic field of a PMQ triplet with respect to the transverse axis of an electron beam is illustrated in figure 9(a). Distorted magnetic fields can be caused by misalignment of the entire PMQ triplet assembly with respect to the beam line axis (figure 9(b)) and of the individual quadrupoles with respect to each other (figure 9(c)). In the first case, GEANT4 simulations show that the beamlet distribution becomes noticeably affected when the axis of the triplet assembly is rotated as a whole by more than 0.1 rad with respect to the beam line axis, as shown in figure 9(d). In practice, the triplet can be readily aligned with better precision and this source of error is unlikely to appear. Moreover, the resulting angular displacement of the beamlets would be independent of energy.

On the other hand, small misalignment of each quadrupole within the triplet can have a large effect. A quadrupole where the magnetic field orientation is rotated by as little as 0.01 rad is enough to produce a visible diagonal misalignment of the beamlets' overall arrangement, as shown in figure 9(e) (this is also evident in figure 6(c)), which simulates the effect of a small clockwise rotation around the beam line axis of a single quadrupole, while keeping the other two fixed. At high energies the beamlets' slanting angle decreases, since quadrupoles become less effective in deflecting the electrons. Among the three PMQs, the middle quadrupole produces the highest skew angle since its effective length is almost twice as long as the other two quadrupoles. Although the overall structure of the beamlets is modified by the rotational error, the beamlet size and separation are not significantly affected. In the experiment, all pepper-pot images are skewed by an angle varying between 0.03 and 0.2 rad, indicating that the quadrupoles should be more finely aligned with respect to each other.

6. Conclusions

In conclusion, laser-driven electron beams have been characterized with a PMQ triplet and a pepper-pot mask. For small energy spreads, this setup can directly measure the beam transverse emittance after propagation through the quadrupoles. For large energy spreads, the longitudinal and transverse properties of the beam become coupled, leading to beamlets too broad and distorted to be detectable. The emittance before and after the triplet can still be estimated if the divergence is known. Double bunches are also detected due to inherent energy dependence of

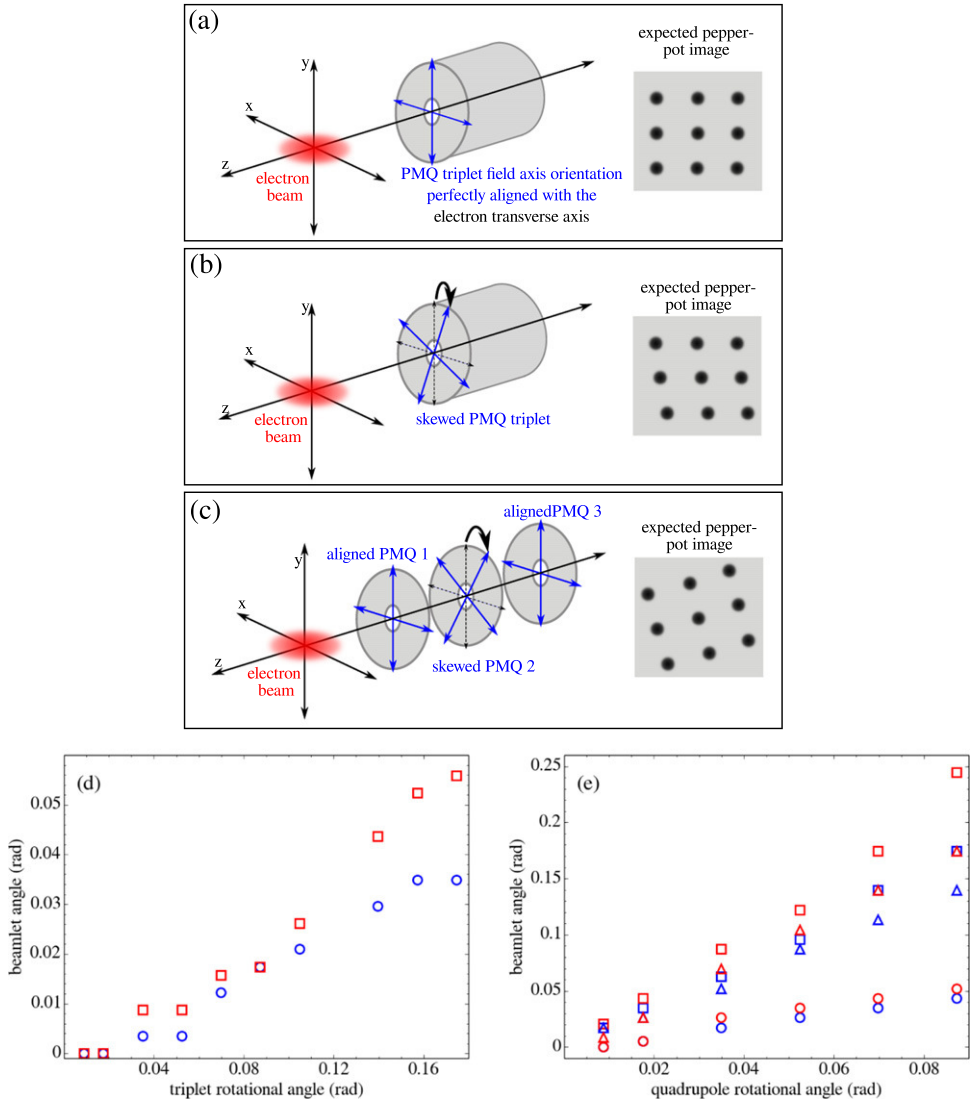

Figure 9. (a) Schematics of a PMQ triplet with magnetic fields axes (blue arrows) perfectly aligned with the electron beam transverse axis, resulting in a well-aligned beamlets. Illustrations of a skewed (b) entire PMQ triplet assembly and (c) individual quadrupole. Beamlets' alignment dependence on the rotational misalignment of (d) the entire PMQ triplet assembly and (e) an individual quadrupole. Blue/red is for horizontal/vertical axis. In (e) different symbols indicate the rotated quadrupole: circle- PMQ1; square- PMQ2; triangle: PMQ3.

the system imaging magnification. Bunches of similar energy can be resolved if their pointing angle difference leads to significantly separated trajectories through the triplet and pepper-pot system. In addition, misalignments of the quadrupole magnets can induce tilt and rotation of the beamlets, making this device a useful diagnostic to fine tune magnetic elements. Real-time triplet optimization could be achieved with independent remote rotational and translational adjustment of each quadrupole.

Due to electron beam pointing fluctuations, most of the outer beamlets are clipped on the detector. Improving the pepper-pot and imaging system to capture the entire beamlet

distribution can provide an absolute value of the electron beam charge as well as the transverse emittance of individual bunches in the double bunch case. Moreover, remotely varying the drift separation (*A* and *B* parameters) between the quadrupoles can induce more variation in the system magnification, leading to precise determination of the central energy of each electron bunch which enhances the PMQ/pepper-pot system as a powerful tool for studying injection and acceleration of multiple bunches in laser wakefields.

Acknowledgements

We acknowledge the support of the UK EPSRC (grant no. EP/J018171/1), the EC's LASERLAB-EUROPE (grant agreement no. 284464, Seventh Framework Programme), EuCARD-2 (grant no. 312453, FP7) and the Extreme Light Infrastructure (ELI) European Project. We also thank David Clark and Tom McCanny for technical support.

References

[1] Esarey E, Schroeder C B and Leemans W P 2009 *Rev. Mod. Phys.* **81** 1229
[2] Rousse A *et al* 2004 *Phys. Rev. Lett.* **93** 135005
[3] Jaroszynski D A *et al* 2006 *Phil. Trans. R. Soc.* A **364** 689
[4] Cipiccia S *et al* 2011 *Nat. Phys.* **7** 867
[5] Schlenvoigt H P *et al* 2007 *Nat. Phys.* **4** 130
[6] Fuchs M *et al* 2009 *Nat. Phys.* **5** 826
[7] Anania M P *et al* 2014 *Appl. Phys. Lett.* **105** 264102
[8] Lim J K, Frigola P, Travish G, Rosenzweig J B, Anderson S G, Brown W J, Jacob J S, Robbins C L and Tremaine A M 2005 *Phys. Rev. ST Accel. Beams* **8** 072401
[9] Becker S *et al* 2009 *Phys. Rev. ST Accel. Beams* **12** 102801
[10] Weingartner R *et al* 2011 *Phys. Rev. ST Accel. Beams* **14** 052801
[11] Sears C M S, Buck A, Schmid K, Mikhailova J, Krausz F and Veisz L 2010 *Phys. Rev. ST Accel. Beams* **13** 092803
[12] Brunetti E *et al* 2010 *Phys. Rev. Lett.* **105** 215007
[13] Weingartner R *et al* 2012 *Phys. Rev. ST Accel. Beams* **15** 111302
[14] Leemans W P *et al* 2006 *Nat. Phys.* **2** 696
[15] Clayton C E *et al* 2010 *Phys. Rev. Lett.* **105** 105003
[16] Walker P A *et al* 2013 *New J. Phys.* **15** 045024
[17] Lundh O, Rechatin C, Lim J, Malka V and Faure J 2013 *Phys. Rev. Lett.* **110** 065005
[18] Yan W C *et al* 2014 *Proc. Natl Acad. Sci. USA* **111** 5825
[19] Islam M R *et al* 2014 *Nat. Phys.* submitted
[20] Popp A *et al* 2010 *Phys. Rev. Lett.* **105** 215001
[21] Wiedemann H 2007 *Particle Accelerator Physics* (New York: Springer)
[22] Anania M P *et al* 2009 *Proc. SPIE* **7359** 735916
[23] Zhang M 1996 Emittance formula for slits and pepper-pot measurement *Technical Report* FERMILAB-TM 1988 (http://inis.iaea.org/search/search.aspx?orig_q=RN:28018451)
[24] Agostinelli S *et al* 2003 *Nucl. Instrum. Methods Phys. Res.* A **506** 250
[25] Wiggins S M *et al* 2010 *Plasma Phys. Control. Fusion* **52** 124032
[26] Meadowcroft A, Bentley C and Stott E 2008 *Rev. Sci. Instrum.* **79** 113102
[27] Ciocarlan C, Wiggins S M, Islam M R, Ersfeld B, Abuazoum S, Wilson R, Aniculaesei C, Welsh G H, Vieux G and Jaroszynski D A 2013 *Phys. Plasmas* **20** 093108